Perfectly conducting cylinder covered by two layers of dielectric separated by an infinitely thin impedance layer: multiple suppression of the scattered field harmonics (rigorous

Research Article | Vol. 31, No. 5 / 27 Feb 2023 / Optics Express 7863

Optics EXPRESS

Perfectly conducting cylinder covered by two layers of dielectric separated by an infinitely thin impedance layer: multiple suppression of the scattered field harmonics (rigorous approach)

YURY SHESTOPALOV[1,5] AND LADISLAU MATEKOVITS[2,3,4,*]

[1] *Faculty of Engineering and Sustainable Development, University of Gävle, Sweden*
[2] *Department of Electronics and Telecommunications, Politecnico di Torino, 10129 Turin, Italy*
[3] *Department of Measurements and Optical Electronics, Politehnica University Timisoara, 300006 Timisoara, Romania*
[4] *Istituto di Elettronica e di Ingegneria dell'Informazione e delle Telecomunicazioni, National Research Council, 10129 Turin, Italy*
[5] *yuyshv@hig.se*
[*] *ladislau.matekovits@polito.it*

Abstract: We propose and develop a novel rigorous technique that enables one to obtain the explicit numerical values of parameters at which several lowest-order harmonics of the scattered field are suppressed. This provides partial cloaking of the object, a perfectly conducting cylinder of circular cross section covered by two layers of dielectric separated by an infinitely thin impedance layer, a two-layer impedance Goubau line (GL). The developed approach is a rigorous method that enables one to obtain in the closed form (and without numerical calculations) the values of parameters providing the cloaking effect, achieved particularly in terms of the suppression of several scattered field harmonics and variation of the sheet impedance. This issue constitutes the novelty of the accomplished study. The elaborated technique could be applied to validate the results obtained by commercial solvers with virtually no limitations on the parameter ranges, i.e., use it as a benchmark. The determination of the cloaking parameters is straightforward and does not require computations. We perform comprehensive visualization and analysis of the achieved partial cloaking. The developed parameter-continuation technique enables one to increase the number of the suppressed scattered-field harmonics by appropriate choice of the impedance. The method can be extended to any dielectric-layered impedance structures possessing circular or planar symmetry.

1. Introduction

Field manipulation has been a hot topic in the research panorama of the last decades. One of the most challenging applications is represented by the possibility to hide objects to the interrogating incident field, being this electrical, acoustic, thermal, or other. Cloaking has always been seen as "magic", and so understanding it has fascinated the research community. Different explanations have been provided, and during the years theories as plasmonic cloaking [1], transformation optics [2,3] or scattering cancellation theory further enriched by mantle cloaking [4], have been proposed. Security and sensitivity enhancement are just two of the many applications that could efficiently exploit such phenomenon. However, design and analysis of the right coating has encountered significant problems, and closed-form solutions are not always available. Analytical expressions are given for canonical geometries, and for relatively simple coating structures, such as a single-layer coverage [5–7].

#473217 https://doi.org/10.1364/OE.473217
Journal © 2023 Received 14 Aug 2022; revised 12 Dec 2022; accepted 12 Dec 2022; published 17 Feb 2023

Optics EXPRESS

The possibility to design devices with reduced scattering has intrigued and keep intriguing the optical community for decades, with several applications, like imaging, [8], high-Q optical resonators [9], perfect lens [10], and other challenging applications on terahertz regime [11].

Depending on the nature of the materials involved for the core object with desired reduced scattering (metals or dielectrics), the electromagnetic energy can be re-routed around an obstacle by means of inhomogeneous and anisotropic cloaking shells as in Transformation Optics [2,3] or let the waves pass through the object-cloak pair without any distortion as in scattering cancellation approaches [1]. As an important result taken from the literature of imaging problems [12], the visibility of a generic object depends on the number M of degrees of freedom of the scattered fields and, in order to reduce its scattering, there is the need to deal with the suppression of the same number M of independent harmonics radiating in the background scenario.

In quasi-static regime, where the object is very small compared to the incoming wavelength, it has been sufficient to consider $M = 1$ to take the overall control on scattered fields and to enforce a single-dominant harmonic cancellation with a single volumetric metamaterial coating [1] or a single thin impedance metasurface, namely mantle cloaking [4]. When the scattering is dominated by one harmonic wave ($M = 1$), a single harmonic wave cancellation is sufficient for effective scattering reduction: this happens in quasi-static regime for the lowest order harmonic wave, even if single-dominant scattering approximations can hold in other frequency regimes as well. However, when the scattering is dominated by two or more harmonic waves ($M>2$), single-harmonic suppression is no more enough and advanced multi-harmonics mantle cloaks are needed for controlling the desired scattering reduction.

In this paper, we propose a general methodology for cloaking by enforcing only given set M of independent harmonics for scattering suppression: in addition, this will be performed in a more general framework considering metallic cylinders.

Simplified models however cannot be sufficient when description of the field propagation in a more realistic media is of interest; bandwidth issues and availability of accurate materials and associated technical solutions, including technology to be used to realize the necessary coatings are other aspects that limit the applications of the available solutions described in scientific literature. Extension to multilayer coatings for example is only spuriously presented. The present work aims to answer to some of the open problems related to the study of multilayer configurations, targeting cloaking of cylindrical symmetry; an implanted bio-metallic cylinder used for hip implant is a possible example. The use of such a medical device is mandatory in case of severe damage of bones following injury. Elderly people are also sensitive to this problem. When people with implants are travelling, for example, their airport checking is more time consuming, and the use of screening is also subject to special procedure. The presence of other implants, e.g., metallic dental ones, also requires special attention for MRI investigation, or others.

In particular, in the present investigation an analytical solution for a multilayer configuration is proposed aiming to cancel different higher-order harmonics of the scattered field. The rigorous approach is proposed for the first time and paves the way for future extensions on the same line. In particular, the cancellation of one harmonic obtained using a single-layer coating is extended, offering a general framework to cancel three, four, or even a larger amount of harmonics. Such complex appearances happen when specific conditions are fulfilled. These conditions are developed, and the analytic solutions are supported by plots of the 2D scattered field distributions around the metallic cylinder. Machine-precision numerical results are reported, demonstrating the correctness of the method.

During recent years, the authors of the present work have already proposed various solutions for the problem related to the present topic: analytical solution based on one of the Devaney-Wolf theorems [13], tunable cloaking, [14], analytical formulation based on the contrast formulation [15] or put in evidence the presence of anapole modes [16] in association with the presence of

Optics EXPRESS

cloaking. A theoretical approach has been elaborated [5] that enables one obtain in the closed form the expression for the parameters at which several lowest-order scattered-field harmonics are eliminated. This paper is a continuation of these studies.

To outline basic features of the developed research technique, consider scattering of a plane wave by a perfectly conducting cylinder (PEC) of circular cross section with a radius a covered by two layers of dielectric separated by an infinitely thin impedance layer (placed between the dielectric layers on a circle $r = a_1$ as shown in Fig. 1). This structure may be conditionally called a two-layer impedance Goubau line (GL).

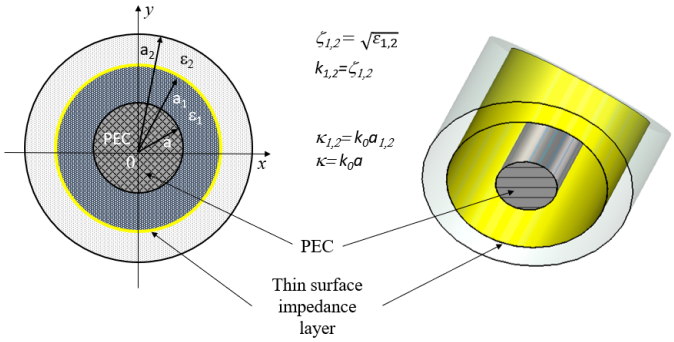

Fig. 1. A two-layer impedance Goubau line.

A goal of this study is, proceeding from the above scattering problem, to rigorously determine the values of parameters at which several (three, five, or more) lowest harmonics of the scattered field are cancelled; the research technique is a substantial extension of the method developed in [5]. The question is to obtain the explicit numerical values of parameters at which the coefficients multiplying several first lowest-order harmonics vanish. The goal is achieved by investigating functional properties of coefficients considering them as vector-functions (maps) of several real and complex variables and proving that the corresponding system is solvable. This requires application of fine mathematical analysis and calculations that cannot be performed using commercial solvers. In addition, the difficulty is in the complicated form of the expression for the coefficients (similar to eq. (5) from [17] or formula (10) below).

Cylindrical scatterers having circular cross-sectional symmetry can be characterized by finitely many parameters. For the basic structures like a PEC, a dielectric rod (DR), and a PEC of circular cross section covered by a concentric circular layer of homogeneous dielectric, a GL, the problem of partial cloaking and invisibility has been efficiently solved [5–7]. Using the theory of generalized cylindrical polynomials (GCPs) [18,19] the parameter sets have been determined when partial cloaking or partial invisibility is observed due to the suppression of several (up to five) principal scattered-field harmonics. In fact, for single- and multilayer DRs and GLs (and other obstacles with circular symmetry), the scattered-field expansion coefficients have a definite structure involving GCPs. This fact made it possible to prove the existence, determine the localization and efficiently calculate zeros and singularities of the expansion coefficients verifying and studying thus partial cloaking and invisibility.

The method characterized above in its background is close to that in [5]; however, the technical and mathematical difficulties connected with the analysis of this impedance structure are so significant that it requires a separate study.

A two-layer impedance GL can be fully characterized by a set of five dimensionless parameters (radii of cylinders and permittivities of the dielectrics filling the layers). Inserting an infinitely thin impedance layer on the boundary between two dielectric layers adds one more such parameter and enables one to achieve and control multiple suppression of harmonics. In fact, we have shown

Optics EXPRESS

that for the three GL parameters being fixed (and determined according to explicit formulas in (29) below) and every value of the relative PEC radius κ taken from a certain interval (determined explicitly) and permittivity $\epsilon_1>1$ of the internal dielectric layer, (a) there is exactly one value of surface impedance that provides the triple suppression of the three lowest-order (principal) scattered-field harmonics, and (b) for every real surface impedance value, there is a κ such that the three lowest-order scattered-field harmonics are suppressed for any value of the permittivity of the internal dielectric layer $\epsilon_1>1$.

Moreover, the coefficients specifying the scattered field in the external domain are, up to a factor, real-valued quantities and linear functions with respect to the surface impedance which enables one to explicitly determine the (real) impedance values that yield multiple suppression.

All the parameter values that provide multiple suppression of the lowest-order scattered-field harmonics can be calculated explicitly using closed-form expressions.

Further increase of the number of suppressed harmonics can be achieved directly by simultaneous analysis of the dependence of the surface impedance on parameters for different indices of harmonics (given by formula (31) below). A two-layer impedance GL may be considered therefore as a cloaking device where the impedance layer governs cloaking or invisibility for wider parameter sets and in broader spatial domains.

Another important conclusion is that the obtained explicit numerical values at which the lowest-order scattered-field harmonics are eliminated may be considered as absolute constants inherent to the specific scatterer (e.g. a two-layer impedance GL) similar to cut-off frequencies or normal-wave propagation constants of a circular waveguide or DR.

2. Series solution

For a two-layer impedance GL where the dielectric layers are filled with the media having relative permittivities ϵ_1 and ϵ_2 (respectively, the internal and external layers, as shown in Fig. 1), the solution to the problem of the plane electromagnetic wave diffraction is sought, for the single nonzero electric field component $u(r,\varphi)$ where (r,φ) are the polar coordinates of the observation point, in the form [7]

$$u(r,\varphi)=\begin{cases}\sum_{n=-\infty}^{\infty} A_n u_{n1}(k_1 r)\, e^{in\varphi}, & a<r<a_1,\\ \sum_{n=-\infty}^{\infty} [B_n J_n(k_2 r)+C_n Y_n(k_2 r)]\, e^{in\varphi}, & a_1<r<a_2,\\ \sum_{n=-\infty}^{\infty} D_n H_n^{(1)}(k_0 r)\, e^{in\varphi}, & r>a_2;\end{cases} \tag{1}$$

here $\kappa = k_0 a$ and $\kappa_{1,2} = k_0 a_{1,2}$ are dimensionless parameters, $k_0 = \omega/c$ is the free-space wavenumber (c is the speed of light in vacuum), and

$$u_{n1}(k_1 r) = J_n(k_1 r) - \alpha_{n1} Y_n(k_1 r),\ \alpha_{n1} = \frac{J_n(\kappa\zeta_1)}{Y_n(\kappa\zeta_1)} = \frac{J_n(z)}{Y_n(z)},\ k_{1,2} = k_0\zeta_{1,2},\ \zeta_{1,2} = \sqrt{\epsilon_{1,2}}, \tag{2}$$

where $z=\kappa\zeta_1$, so that $u_{n1}(k_1 r)$ satisfies the boundary condition $u_{n1}(k_1 a)=0$ on the PEC surface. Using formulas (43) from Appendix and setting $w=\kappa_1\zeta_1$, we obtain a quantity

$$\begin{aligned} u_{n1}(k_1 a_1) &= J_n(k_1 a_1) - \alpha_{n1} Y_n(k_1 a_1) = J_n(\kappa_1\zeta_1) - \alpha_{n1} Y_n(\kappa_1\zeta_1) = \\ &= \frac{1}{Y_n(z)}\left[J_n(w)\, Y_n(z) - J_n(z) Y_n(w)\right] = \frac{p_n(w,z)}{Y_n(z)} \end{aligned} \tag{3}$$

which will be used below in the formulas for the expansion coefficients.

Note that in actual calculations using (1) we take only several leading series terms, e.g.

$$u(r,\varphi) \approx \tilde{u}(r,\varphi) = \sum_{n=-N}^{N} D_n H_n^{(1)}(k_0 r)\, e^{in\varphi}, \quad r>a_2, \tag{4}$$

where $N \sim 10$ because the series term rapidly decays.

Optics EXPRESS

Next, if the $L = 2l + 1 \geq 1$ lowest-order scattered-field harmonics are eliminated (suppressed), e.g. three with the indices $n = -1, 0, 1$ when $L = 3$ and $l = 1$, then the 'suppressed' part involving the eliminated harmonics (series terms) vanishes, $\tilde{u}^{(L)}(r, \varphi) = 0$, where

$$\begin{aligned} \tilde{u}(r, \varphi) &= \tilde{u}^{(L)}(r, \varphi) + \tilde{u}^{(M)}(r, \varphi), \\ \tilde{u}^{(L)}(r, \varphi) &= \sum_{n=-l}^{l} D_n H_n^{(1)}(k_0 r)\, e^{in\varphi}, \\ \tilde{u}^{(M)}(r, \varphi) &= \sum_{n=-M}^{-(l+1)} D_n H_n^{(1)}(k_0 r)\, e^{in\varphi} + \sum_{n=l+1}^{M} D_n H_n^{(1)}(k_0 r)\, e^{in\varphi} \quad (r{>}a_2). \end{aligned} \tag{5}$$

According to Parseval's equality which gives the squared L_2-norm of the function $u(r, \varphi)$ given for $r{>}a_2$ by the third line in (1)

$$\|u(r, \varphi)\|_2^2 = \int_0^{2\pi} |u(r, \varphi)|^2\, d\varphi = 2\pi \sum_{n=-\infty}^{\infty} \left| D_n H_n^{(1)}(k_0 r) \right|^2, \; r{>}a_2, \tag{6}$$

the quantity

$$U(r) = \sum_{n=-N}^{N} \left| D_n H_n^{(1)}(k_0 r) \right|^2, \; r{>}a_2, \tag{7}$$

may serve as a correct measure of the radial distribution of the intensity of the electromagnetic scattered-field component, demonstrating a sharp fall when several lowest-order harmonics are suppressed.

Application of the transmission conditions on the circles $r = a_1$ and $r = a_2$

$$\begin{gathered} u(r = a_1 - 0, \varphi) = u(r = a_2 + 0, \varphi), \\ Z\left(\frac{\partial u}{\partial r}(r = a_1 + 0, \varphi) - \frac{\partial u}{\partial r}(r = a_1 - 0, \varphi) \right) = u(r = a_1 - 0, \varphi), \\ u(r = a_2 - 0, \varphi) - u(r = a_2 + 0, \varphi) = u_0(a_2, \varphi), \\ \frac{\partial u}{\partial r}(r = a_2 - 0, \varphi) - \frac{\partial u}{\partial r}(r = a_2 + 0, \varphi) = \frac{\partial u_0}{\partial r}(a_2, \varphi), \end{gathered}$$

where $u_0(r, \varphi) = \sum_{n=-\infty}^{\infty} i^{-n} J_n(k_0 r)\, e^{in\varphi}$, yields a linear equation system

$$A\mathbf{X} = \mathbf{F}$$

for the determination of unknown coefficients $A_n,\ B_n,\ C_n,\ D_n$; a 4×4 system matrix

$$A = \begin{pmatrix} u_{n1}(k_1 a_1) & -J_n(\kappa_1 \zeta_2) & -Y_n(\kappa_1 \zeta_2) & 0 \\ v_{n1}(k_1 a_1) & -Zk_2 J_n'(\kappa_1 \zeta_2) & -Zk_2 Y_n'(\kappa_1 \zeta_2) & 0 \\ 0 & J_n(\kappa_2 \zeta_2) & Y_n(\kappa_2 \zeta_2) & -H_n^{(1)}(\kappa_2) \\ 0 & \zeta_2 J_n'(\kappa_2 \zeta_2) & \zeta_2 Y_n'(\kappa_2 \zeta_2) & -\left(H_n^{(1)}(\kappa_2) \right)' \end{pmatrix} \tag{8}$$

where, according to (3),

$$\begin{aligned} v_{n1}(k_1 a_1) &= u_{n1}(k_1 a_1) + Zk_1 u_{n1}'(k_1 a_1) = \\ &= J_n(\kappa_1 \zeta_1) + Zk_1 J_n'(\kappa_1 \zeta_1) - \alpha_{n1} \left(Y_n(\kappa_1 \zeta_1) + Zk_1 Y_n'(\kappa_1 \zeta_1) \right) = \\ &= \tilde{Z}_n J_n(\kappa_1 \zeta_1) - Zk_1 J_{n+1}(\kappa_1 \zeta_1) - \alpha_{n1} \left[\tilde{Z}_n Y_n(\kappa_1 \zeta_1) - Zk_1 Y_{n+1}(\kappa_1 \zeta_1) \right] = \\ &= \tilde{Z}_n u_{n1}(k_1 a_1) - Zk_1 u_{n+1,1}(\kappa_1 \zeta_1), \end{aligned} \tag{9}$$

Optics EXPRESS

$\tilde{Z}_n = 1 + \hat{Z}\frac{n}{\kappa_1}$, $\hat{Z} = k_0 Z$, $u_{n+1,1}(\kappa_1\zeta_1) = J_{n+1}(\kappa_1\zeta_1) - \alpha_{n1}Y_{n+1}(\kappa_1\zeta_1)$, and the vectors of unknowns and the right-hand side

$$\mathbf{X} = [A_n,\ B_n,\ C_n,\ D_n]^T,\ \mathbf{F} = [0,\ 0,\ i^{-n}J_n(\kappa_2),\ i^{-n}J_n'(\kappa_2)]^T.$$

Coefficients $A_n,\ B_n,\ C_n,\ D_n$ can be determined using the Cramer rule; for D_n we have

$$\det A \cdot D_n = D_n^{(1)} = i^{-n}\begin{vmatrix} u_{n1}(k_1a_1) & -J_n(\kappa_1\zeta_2) & -Y_n(\kappa_1\zeta_2) & 0 \\ v_{n1}(k_1a_1) & -Zk_2J_n'(\kappa_1\zeta_2) & -Zk_2Y_n'(\kappa_1\zeta_2) & 0 \\ 0 & J_n(\kappa_2\zeta_2) & Y_n(\kappa_2\zeta_2) & J_n(\kappa_2) \\ 0 & \zeta_2J_n'(\kappa_2\zeta_2) & \zeta_2Y_n'(\kappa_2\zeta_2) & J_n'(\kappa_2) \end{vmatrix} = \tag{10}$$
$$= i^{-n}\left[-Zk_2u_{n1}(k_1a_1)d_{n1} + v_{n1}(k_1a_1)d_{n2}\right],$$

where the determinants

$$d_{n1} = \begin{vmatrix} J_n'(\kappa_1\zeta_2) & Y_n'(\kappa_1\zeta_2) & 0 \\ J_n(\kappa_2\zeta_2) & Y_n(\kappa_2\zeta_2) & J_n(\kappa_2) \\ \zeta_2J_n'(\kappa_2\zeta_2) & \zeta_2Y_n'(\kappa_2\zeta_2) & J_n'(\kappa_2) \end{vmatrix} = -\zeta_2J_n(\kappa_2)s_n(x,y) + J_n'(\kappa_2)r_n(x,y),$$

$$d_{n2} = \begin{vmatrix} J_n(\kappa_1\zeta_2) & Y_n(\kappa_1\zeta_2) & 0 \\ J_n(\kappa_2\zeta_2) & Y_n(\kappa_2\zeta_2) & J_n(\kappa_2) \\ \zeta_2J_n'(\kappa_2\zeta_2) & \zeta_2Y_n'(\kappa_2\zeta_2) & J_n'(\kappa_2) \end{vmatrix} = -\zeta_2J_n(\kappa_2)q_n(x,y) + J_n'(\kappa_2)p_n(x,y)$$

are represented using standard notations (39–42) for cross-products and the variables $x = \kappa_1\zeta_2$ and $y = \kappa_2\zeta_2$.

Thus, the coefficient

$$D_n = \frac{D_n^{(1)}}{D_n^{(2)}},\quad D_n^{(2)} = \det A, \tag{11}$$

where, up to a factor i^{-n}, $D_n^{(1)}$ is a real-valued quantity having the form of a weighted sum of products of cross-products of cylindrical functions [18]. Such sums are referred to as generalized cylindrical polynomials (GCPs) and their theory is developed in [19].

3. Multiple suppression of harmonics: functional approach

3.1. General setting

Fourier coefficients $A_n,\ B_n,\ C_n$, and D_n specifying, as in (1), the solution to the problem of the plane electromagnetic wave diffraction for a two-layer impedance GL (or any other cylindrical structure possessing circular symmetry) are functions of the problem parameters.

One can state a problem to determine the parameter sets such that several coefficients of the same group ($A_n,\ B_n,\ C_n$, or D_n) corresponding to the particular spatial region vanish simultaneously. In particular, D_n specify the scattered-field harmonics in the domain outsied the scatterer.

To this end, let us introduce the parameter vectors $\mathbf{w}$ and $\mathbf{v}$ comprising all the parameters of a particular structure. For a PEC of circular cross section with (internal) radius a covered by two layers of dielectric separated by an infinitely thin impedance layer (placed between the dielectric layers on a circle $r = a_1$) and external radius a_2, we have the parameter vectors

Optics EXPRESS

$\mathbf{w} = \{w_j\}_{j=1}^{6} = (Z, \kappa, \kappa_1, \kappa_2, \zeta_1, \zeta_2)$ and $\mathbf{v} = \{v_j\}_{j=1}^{7} = (Z, \omega, a, a_1, a_2, \zeta_1, \zeta_2)$ of, respectively, dimensionless (except for impedance Z) and dimensional quantities. Next, one can consider the numerators of coefficients D_n, $D_n^{(1)} = D_n^{(1)}(\mathbf{w})$ or $D_n^{(1)} = D_n^{(1)}(\mathbf{v})$ as functions of several variables, real or complex. If $\mathbf{w} = \mathbf{w}^*$ or $\mathbf{v} = \mathbf{v}^*$ solves the system of $m + 1$ equations

$$D_n^{(1)}(\mathbf{w}) = 0 \quad \text{or} \quad D_n^{(1)}(\mathbf{v}) = 0, \quad n = 0, 1, 2, \dots m, \ m = 0, 1, 2, \dots, \tag{12}$$

then the corresponding $2m + 1$ scattered-field harmonics are eliminated (suppressed).

The set of coefficients involved in system (12) form in its turn a vector $\mathbf{D}_m^{(1)} = \left\{D_n^{(1)}\right\}_{n=1}^{m+1}$ and may be considered as a map $\mathbf{D}_m^{(1)}(\mathbf{w}) : \mathrm{R}^{N_w} \to \mathrm{R}^{m+1}$ or $\mathbf{D}_m^{(1)}(\mathbf{v}) : \mathrm{R}^{N_v} \to \mathrm{R}^{m+1}$ ($m+1$-dimensional vector-functions of $N_{w,v}$ real or complex variables). For a two-layer impedance GL, $N_w = 6$ and $N_v = 7$.

3.2. Explicit determination of parameters providing multiple suppression for a two-layer impedance GL

Parameter sets that give explicit (reference) solutions to a particular equation of system (12) with a fixed index n may be called, respectively, reference couples (RCs) and reference triples (RTs). RCs $\mathbf{w}^* = \left(\kappa_{(m)}^{(n)}, (\zeta_{(l,m)}^{(n)})^2\right)$ for DR and RTs $\mathbf{w}^* = \left(\kappa_{(m)}^{(n)}, \kappa_{1,(m,p,s)}^{(n)}, (\zeta_{(m,s)}^{(n)})^2\right)$ for GL have been determined in [5]; they are given below in formulas (37) and (38).

Make use of the methods developed in [5,19] and determine explicitly the parameter sets providing multiple suppression for a two-layer impedance GL.

In view of the relations [18], 9.1.5, that couple the Bessel and Neumann functions with the 'opposite' orders $J_{-n}(x) = (-1)^n J_n(x)$ and $Y_{-n}(x) = (-1)^n Y_n(x)$, $D_{-n}^{(1)}$ coincides, up to a factor $(-1)^m$ for a certain integer m, with $D_n^{(1)}$ ($n = 1, 2, \dots$).

One can rewrite the expression for $D_n^{(1)}$ in the form

$$\begin{aligned}\tilde{D}_n^{(1)} &= i^n D_n^{(1)} \\ &= -Zk_2 u_{n1}(\kappa_1\zeta_1)\left[-\zeta_2 J_n(\kappa_2)s_n + J_n'(\kappa_2)r_n\right] + v_{n1}(\kappa_1\zeta_1)\left[-\zeta_2 J_n(\kappa_2)q_n + J_n'(\kappa_2)p_n\right] \\ &= \zeta_2 J_n(\kappa_2)\left[Zk_2 u_{n1}(\kappa_1\zeta_1)s_n - v_{n1}(\kappa_1\zeta_1)q_n\right] + J_n'(\kappa_2)\left[-Zk_2 u_{n1}(\kappa_1\zeta_1)r_n + v_{n1}(\kappa_1\zeta_1)p_n\right].\end{aligned} \tag{13}$$

In particular, for $n = 0, 1$, using formulas (43) and (3) and setting $z = \kappa\zeta_1$ and $w = \kappa_1\zeta_1$, we obtain

$$u_{01} = \frac{1}{Y_0(z)}\left[J_0(w)Y_0(z) - J_0(z)Y_0(w)\right] = \frac{p_0(w,z)}{Y_0(z)}, \tag{14}$$

$$u_{11} = \frac{1}{Y_1(z)}\left[J_1(w)Y_1(z) - J_1(z)Y_1(w)\right] = \frac{p_1(w,z)}{Y_1(z)}, \tag{15}$$

$$v_{01} = u_{01} - Zk_1 u_{1,1} = \frac{1}{Y_0(z)}\left[p_0(w,z) - Zk_1 I_{1,0}(w,z)\right], \tag{16}$$

$$u_{1,1} = J_1(w) - \alpha_{01}Y_1(w) = \frac{1}{Y_0(z)}\left[J_1(w)Y_0(z) - J_0(z)Y_1(w)\right] = \frac{I_{1,0}(w,z)}{Y_0(z)} \tag{17}$$

$$\tilde{D}_0^{(1)} = \zeta_2 J_0(\kappa_2)\left[Zk_2 u_{01}p_1 - v_{01}q_0\right] - J_1(\kappa_2)\left[-Zk_2 u_{01}r_0 + v_{01}p_0\right], \tag{18}$$

$$\tilde{D}_1^{(1)} = \zeta_2 J_1(\kappa_2)\left[Zk_2 u_{11}s_1 - v_{11}q_1\right] + J_1'(\kappa_2)\left[-Zk_2 u_{11}r_1 + v_{11}p_1\right]. \tag{19}$$

Thus , if $J_1(\kappa_2) = 0$, i.e. $\kappa_2 = \nu_m^1$, $m = 1, 2, \dots$, and $p_1(x, y) = 0$, we have

$$\tilde{D}_0^{(1)} = -\zeta_2 J_0(\nu_m^1)v_{01}q_0, \quad \tilde{D}_1^{(1)} = -Zk_2 J_1'(\nu_m^1)u_{11}r_1. \tag{20}$$

Optics EXPRESS

We have $\tilde{D}_0^{(1)} = 0$ if $v_{01} = 0$ or $q_0(x, y) = 0$; the former condition holds at

$$Z = \frac{p_0(w,z)}{k_1 I_{1,0}(w,z)} = \frac{1}{k_1}\frac{J_0(w)\,Y_0(z) - J_0(z)Y_0(w)}{J_1(w)\,Y_0(z) - J_0(z)Y_1(w)}, \tag{21}$$

Note that the conditions

$$\begin{cases} p_0(w,z) = J_0(w)\,Y_0(z) - J_0(z)Y_0(w) = 0, \\ I_{1,0}(w,z) = J_1(w)\,Y_0(z) - J_0(z)Y_1(w) = 0, \end{cases} \tag{22}$$

which may yield $v_{01} = 0$ are not valid: homogeneous system (22) is not solvable with respect to $J_0(z)$, $Y_0(z)$ because its determinant, a Wronskian $I_{1,0}(w,w) = J_1(w)\,Y_0(w) - J_0(w)Y_1(w) = \frac{2}{\pi w} \neq 0$.

The condition $q_0(x, y) = 0$ holds if

$$J_1(y)\,Y_0(x) - J_0(x)Y_1(y) = 0. \tag{23}$$

Next, $\tilde{D}_1^{(1)} = 0$ if $u_{11} = 0$ or $r_1 = 0$ which holds at

$$p_1(w,z) = J_1(w)\,Y_1(z) - J_1(z)Y_1(w) = 0 \tag{24}$$

or at

$$r_1(x,y) = J_1'(x)\,Y_1(y) - J_1(y)Y_1'(x) = \frac{1}{x}p_1(x,y) + I_{1,2}(y,x) = I_{1,2}(y,x) = 0. \tag{25}$$

Thus $\tilde{D}_0^{(1)} = \tilde{D}_1^{(1)} = 0$ if

$$\begin{cases} \kappa_2 = \nu_m^1, \quad m = 1, 2, \ldots, \\ J_1(x)\,Y_1(\nu_m^1\zeta_2) - J_1(\nu_m^1\zeta_2)Y_1(x) = 0, \\ J_1(w)\,Y_1(z) - J_1(z)Y_1(w) = 0, \\ Z = \dfrac{1}{k_1}\dfrac{J_0(w)\,Y_0(z) - J_0(z)Y_0(w)}{J_1(w)\,Y_0(z) - J_0(z)Y_1(w)} = \dfrac{\pi z}{2k_1}\dfrac{Y_1(z)}{Y_1(w)}\left[J_0(w)\,Y_0(z) - J_0(z)Y_0(w)\right], \end{cases} \tag{26}$$

or

$$\begin{cases} \kappa_2 = \nu_m^1, \quad m = 1, 2, \ldots, \\ J_1(x)\,Y_1(\nu_m^1\zeta_2) - J_1(\nu_m^1\zeta_2)Y_1(x) = 0, \\ J_1\left(\nu_m^1\zeta_2\right)Y_2(x) - J_1(x)Y_2\left(\nu_m^1\zeta_2\right) = 0, \\ Z = \dfrac{1}{k_1}\dfrac{J_0(w)\,Y_0(z) - J_0(z)Y_0(w)}{J_1(w)\,Y_0(z) - J_0(z)Y_1(w)}, \end{cases} \tag{27}$$

or

$$\begin{cases} \kappa_2 = \nu_m^1, \quad m = 1, 2, \ldots, \\ J_1(x)\,Y_1(\nu_m^1\zeta_2) - J_1(\nu_m^1\zeta_2)Y_1(x) = 0, \\ J_1\left(\nu_m^1\zeta_2\right)Y_2(x) - J_1(x)Y_2\left(\nu_m^1\zeta_2\right) = 0, \\ J_1\left(\nu_m^1\zeta_2\right)Y_0(x) - J_0(x)Y_1\left(\nu_m^1\zeta_2\right) = 0, \end{cases} \tag{28}$$

where $x = \kappa_1\zeta_2$, $z = \kappa\zeta_1$, and $w = \kappa_1\zeta_1$. The three latter equations of the latter system comprise six independent quantities $J_0(x)$, $J_1(y)$, $Y_{0,1}(x)$, $Y_{1,2}(y)$ and therefore the system is solvable; the solvability condition is $Y_0(x)Y_1(x)J_1(y)Y_2(y) - J_0(x)Y_2(x)Y_1^2(y) = 0$, $y = \nu_m^1\zeta_2$.

Optics EXPRESS

Consider conditions (system) (27). The second and third equations are satisfied if $J_1(x) = 0$ and $J_1(\nu_m^1\zeta_2) = 0$, i.e. at $\kappa_1\zeta_2 = \nu_l^1$ and $\nu_m^1\zeta_2 = \nu_s^1$ which yield

$$\begin{cases} \kappa_2 = \nu_m^1,\ \kappa_1 = \dfrac{\nu_l^1\nu_m^1}{\nu_s^1},\ \zeta_2 = \dfrac{\nu_s^1}{\nu_m^1},\quad s = m+1, m+2, \dots\ l = 1, 2, \dots s-1,\ m = 1, 2, \dots, \\ Z = Z_{01} = \dfrac{1}{k_1}\dfrac{J_0(w)\,Y_0(z) - J_0(z)Y_0(w)}{J_1(w)\,Y_0(z) - J_0(z)Y_1(w)},\quad w = \beta_{lms}\zeta_1,\ \beta_{lms} = \dfrac{\nu_l^1\nu_m^1}{\nu_s^1}\quad z = \kappa\zeta_1,\quad \kappa<\kappa_1. \end{cases} \tag{29}$$

Note that (29) provide the fulfillment of physically grounded relations $\kappa_1<\kappa_2$ and $\zeta_2>1$ (for standard lossless dielectric medium filling the external ring of an impedance GL) between parameters κ_1, κ_2, and ζ_2.

If relations (29) for $\kappa_1, \kappa_2, \zeta_2$ hold, then the triple suppression of three scattered-field harmonics with the indices $n = 0, \pm1$ takes place at arbitrary values of two parameters κ and ζ_1 and the impedance given by the equality in (29). Here, $0<\kappa<\kappa_1$, $\zeta_1>1$, and $\zeta_2>1$ for a 'standard' lossless media. However, generally, ζ_1 or ζ_2 may be complex quantities.

3.3. Multiple suppression in wider parameter ranges

The availability of closed-form solutions is essential for solving system (12) in wider parameter ranges.

For a two-layer impedance GL, $D_n^{(1)}$ is a linear function of impedance Z according to (10) which yields

$$\begin{aligned} D_n^{(1)} = 0 \quad \text{at} \quad Z &= \frac{v_{n1}(k_1a_1)d_{n2}}{k_2u_{n1}(k_1a_1)d_{n1}} = \\ &= \frac{1}{k_2}\left(1 + \hat{Z}\left[\frac{n}{\kappa_1} - \zeta_1\frac{I_{n+1,n}(w,z)}{p_n(w,z)}\right]\right)\frac{\zeta_2J_n(\kappa_2)q_n(x,y) - J_n'(\kappa_2)p_n(x,y)}{\zeta_2J_n(\kappa_2)s_n(x,y) - J_n'(\kappa_2)r_n(x,y)},\quad n = 0, 1, 2\dots. \end{aligned} \tag{30}$$

The relation for impedance Z in (30) is a linear equation with respect to Z having the form $Z = (1 + AZ)B$ with certain A and B and can be solved to give an explicit expression

$$\begin{aligned} &\hat{Z} = Z_n = \left[\zeta_2\frac{\zeta_2J_n(\kappa_2)s_n(x,y) - J_n'(\kappa_2)r_n(x,y)}{\zeta_2J_n(\kappa_2)q_n(x,y) - J_n'(\kappa_2)p_n(x,y)} + \zeta_1\frac{I_{n+1,n}(w,z)}{p_n(w,z)} - \frac{n}{\kappa_1}\right]^{-1}, \\ &n = 0, 1, 2\dots,\qquad x = \kappa_1\zeta_2,\quad y = \kappa_2\zeta_2,\quad w = \kappa_1\zeta_1,\quad z = \kappa\zeta_1. \end{aligned} \tag{31}$$

This means that at arbitrary values of five parameters forming a vector $\mathbf{u} = (\kappa, \kappa_1, \kappa_2, \zeta_1, \zeta_2)$ (where $\kappa_2>\kappa_1>\kappa>0$), that specify a two-layer impedance GL, the double suppression of two scattered-field harmonics with indices $\pm n$ takes place if equality (30) for the impedance holds. Note that for a 'standard' lossless media, $\zeta_1>1$ and $\zeta_2>1$. However, generally, ζ_1 or ζ_2 may be complex quantities.

The set of impedance values involved in (31) form a vector $\mathbf{Z} = \{Z_{n_j}\}_{j=1}^m$ and may be considered as a map $\mathbf{Z}(\mathbf{u}) : \mathrm{R}^5 \to \mathrm{R}^m$ (so that $\mathbf{Z}$ is an m-dimensional vector-function of 5 real or complex variables). If, at certain values of parameters, $Z_j = Z_l$ for different nonzero indices $j \neq l$ then four scattered-field harmonics with indices $\pm j$ and $\pm l$ are suppressed. Generally, if the parameter vector $\mathbf{u} = \mathbf{u}^*$ solves the system of m equations $Z_{n_1} = Z_{n_2} = \dots = Z_{n_m}$ for different indices n_j, $j = 1, 2\dots, m$, then $2m$ scattered-field harmonics with indices $\pm n_j$, $j = 1, 2\dots, m$, are suppressed simultaneously.

A particularly important case is the suppression of $2m + 1$ lowest-order (principal) harmonics with indices $0, \pm1, \pm2, \dots, \pm m$ ($m = 1, 2\dots$). To determine the conditions of mutiple suppression of $2m + 1$ lowest-order harmonics it is necessary to solve the system $Z_0(\mathbf{u}) = Z_1(\mathbf{u}) = \dots = Z_m(\mathbf{u})$ of $m + 1$ equations.

Optics EXPRESS

Specific conditions of mutiple suppression can be determined by considering $Z_n = Z_n(\kappa)$ with respect to one parameter, e.g. κ and other, $\kappa_1, \kappa_2, \zeta_1, \zeta_2$, being fixed for several indices n. The points of intersection of $Z_{n'}$ and $Z_{n''}$ with different indices will indicate multiple suppression of four harmonics.

This task may be simplified by finding, as in Section 3.2, parameter sets that give explicit (reference) particular solutions to this system (RCs or RTs).

To this end, consider conditions (29). The relation for impedance Z in (29) means that at the values of parameters κ_1, κ_2, and ζ_2 given in (29),

$$\kappa_2 = \kappa^{(01)}_{2,(m)} = \nu^1_m, \quad \zeta_2 = \zeta^{(01)}_{2,(s,m)} = \frac{\nu^1_s}{\nu^1_m} \ (s{>}m), \quad \kappa_1 = \kappa^{(01)}_{1,(l,m,s)} = \frac{\nu^1_l \nu^1_m}{\nu^1_s} \ (l{<}s) \tag{32}$$

for $m = 1, 2, \ldots$, the triple suppression of the three lowest order scattered-field harmonics with the indices $n = 0, \pm 1$ takes place at arbitrary κ (with $\kappa_2{>}\kappa_1{>}\kappa{>}0$) and ζ_1 if the equality in (29) for the impedance holds. This result is concretized below in Statement 3.3.

The impedance $Z = Z_{01}(\kappa, \zeta_1)$ in (29) may be considered as a function of two independent variables, both real, or real (κ) and complex (ζ_1). If $Z = Z_{01}(\kappa, \zeta_1)$ given by (29) coincide, at certain κ and ζ_1, with $Z = Z_n(\kappa, \zeta_1)$ given by (31) and calculated at $\kappa_2 = \kappa^{(01)}_{2,(m)}$, $\zeta_2 = \zeta^{(01)}_{2,(s,m)}$, and $\kappa_1 = \kappa^{(01)}_{1,(l,m,s)}$ given by (32) (the values of κ_2, ζ_2, and κ_1 are determined according to (29) then five first lowest-order scattered-field harmonics of a two-layer impedance GL with the indices $n = 0, \pm 1, \pm 2$ are suppressed (eliminated).

Note that in the real domain $0{<}\kappa{<}\kappa_1$, $\zeta_1{>}1$ the impedance $Z = Z_{01}(\kappa, \zeta_1)$ in (29) may go to infinity when its denominator, a cross-product

$$q_0(w, z) = J_1(w)\, Y_0(z) - J_0(z) Y_1(w) = 0, \tag{33}$$

or vanish when its numerator, a cross-product

$$p_0(w, z) = J_0(w)\, Y_0(z) - J_0(z) Y_0(w) = 0, \quad w = \frac{\nu^1_l \nu^1_m}{\nu^1_s}\zeta_1, \quad z = \kappa\zeta_1, \quad \kappa{<}\kappa_1. \tag{34}$$

(see (39) and (43) in Appendix).

Let $p^0_t = p^0_t(w)$ and $q^0_t = q^0_t(w)$, $t = 1, 2, \ldots$, denote (real alternating) zeros of cross-products $p_0 = p_0(z)$ and $q_0 = q_0(z)$ considered as functions of z and given by (33) and (34). For a fixed $\zeta_1{>}1$ and indices l, m, s in (29), if $z = p\ (q)^0_m = p\ (q)^0_m(w_{lms})$, $w_{lms} = \beta_{lms}\zeta_1$, then $\kappa = \kappa^{p\ (q),lms}_t = p\ (q)^0_t(w_{lms})/\zeta_1$ is a zero of $p_0 = p_0(\kappa)$ or $q_0 = q_0(\kappa)$ considered as functions of κ.

If $\kappa^{q,lms}_{t'}{<}\kappa_1{<}\kappa^{q,lms}_{t'+1}$ for a certain $t' = 2, 3, \ldots$, then, considering $Z_{01}(\kappa) = p_0(\kappa)q_0^{-1}(\kappa)$ for $\kappa{<}\kappa_1$ with a given (fixed) κ_1 we see that $Z_{01}(\kappa)$ takes (as a continuous and monotonic function of κ) all real values on the intervals $(\kappa^{q,lms}_j, \kappa^{q,lms}_{j+1})$ between its neighboring singularities for $j \le t'$ (i.e. $j = 1, 2 \ldots t'$) that fall into the interval $(0, \kappa_1)$. Note in addition that $Z_{01}(\kappa)$ is one-to-one function on this interval. Therefore, the following holds:

Statement 1.

(i) For every $\kappa \in (\kappa^{q,lms}_j, \kappa^{q,lms}_{j+1})$ and $\zeta_1{>}1$, there is exactly one value of impedance $Z = Z_{01}(\kappa)$ in (29) that provide (for κ_1, κ_2, and ζ_2 given by (29)) the triple suppression of the three lowest-order (principal) scattered-field harmonics with the indices $n = 0, \pm 1$.

(ii) For every real impedance value Z, there is a $\kappa \in (\kappa^{q,lms}_j, \kappa^{q,lms}_{j+1})$ such that the three lowest-order scattered-field harmonics are suppressed for any $\zeta_1{>}1$ (with κ_1, κ_2, and ζ_2 given by (29)).

Taking into account the properties of cross-products summarized in Appendix, it is easy to determine zeros $\kappa^{p,lms}_t$ and $\kappa^{q,lms}_t$ of $p_0(\kappa)$ and $q_0(\kappa)$. In fact, they form virtually periodic sequences

Optics EXPRESS

with a period close to π/ζ_1, as described in Section 6, so that it is sufficient to determine the first zeros with $t = 1$ and then apply a period shift using formula (44) from Section 6.

In particular, the first four (minimal) zeros of the numerator $p_0(\kappa)$ (34) of $Z_{01}(\kappa)$ at $\kappa_1 = 1.5340$, $\kappa_2 = 5.52$, $\zeta_1 = 3$, and $\zeta_2 = 1.5678$ (corresponding to $l = 1$, $m = 2$, $s = 3$ in (32) are $\kappa_1^{p,123}(w^*) = 0.5023$, $\kappa_2^{p,123}(w^*) = \kappa_1 = 1.5340$, $\kappa_3^{p,123}(w^*) = 2.5778$, and $\kappa_4^{p,123}(w^*) = 3.6235$, and of the denominator $q_0(\kappa)$ (33), $\kappa_1^{q,123}(w^*) = 0.07$, $\kappa_2^{q,123}(w^*) = 1.0497$, $\kappa_3^{q,123}(w^*) = 2.0909$, and $\kappa_4^{q,123}(w^*) = 3.1360$, where $w^* = w_{123} = \beta_{123}\zeta_1$ and $\beta_{123} = \kappa_1$. Note that the distances between the neighboring zeros are $\kappa_2^{p,123} - \kappa_1^{p,123} = 1.0317$, $\kappa_3^{p,123} - \kappa_2^{p,123} = 1.0438$, $\kappa_4^{p,123} - \kappa_3^{p,123} = 1.0457$, $\kappa_3^{q,123} - \kappa_2^{q,123} = 1.0412$, and $\kappa_4^{q,123} - \kappa_3^{q,123} = 1.0451$, which is virtually a constant very close (approach as the zero index increases) to the virtual period $\pi/\zeta_1 = \pi/3 = 1.0472$ of the zero sequences $\left\{\kappa_m^{p,123}(w^*)\right\}$ and $\left\{\kappa_m^{q,123}(w^*)\right\}$.

We have already noted that, according to Section 6 in Appendix, zeros of the numerator and denominator of $Z_{01}(\kappa)$, which are cross-products, perfectly alternate; consequently, $Z_{01}(\kappa)$ is a one-to-one monotonic function similar to tangent and takes all real values on the interval between its singularities, namely, every neighboring zeros of its denominator. Functions $Z_n(\kappa)$ given by (31) have (isolated) singularities and zeros differing from those of $Z_{01}(\kappa)$; therefore, the fact that $Z_{01}(\kappa)$ takes all real values for κ between neighboring zeros of its denominator yields the existence of at least one value of κ such that $Z_n(\kappa) = Z_{01}(\kappa)$ on this interval.

3.3.1. Numerical values of parameters of multiple suppression

In view of physical limitations on the parameters of a two-layer impedance GL, of special interest is to consider the intervals between the first two or three minimal zeros q_t^0, $t = 1, 2, 3$.

Taking into account the physical restrictions imposed on permittivity (refraction index ζ) and the decay of coefficients with respect to n, we conclude that the minimal positive values of the CP components make most sufficient contribution to partial invisibility.

Using the values of the first three (positive) zeros of the Bessel function J_1

$$\nu_1^1 = 3.832,\ \nu_2^1 = 7.016,\ \nu_3^1 = 10.173,$$

we obtain, according to (29) and in order of their increase, the first three values of parameters κ_1, κ_2, and ζ_2 of a two-layer impedance GL

$$\begin{aligned} \kappa_2 &= \kappa_{2,(m)}^{(01)} = \nu_m^1,\ m = 1, 2, 3, \\ \zeta_2 &= \zeta_{2,(s,m)}^{(01)} = \frac{\nu_s^1}{\nu_m^1}, \qquad m = 1, s = 2, 3, \quad m = 2, s = 3, \\ \kappa_1 &= \kappa_{1,(l,m,s)}^{(01)} = \frac{\nu_l^1 \nu_m^1}{\nu_s^1}, \quad l = 1, m = 2, s = 3, \end{aligned} \tag{35}$$

given by

$$\left\{ \begin{array}{c} \kappa_2 :\ \kappa_{2,(1)}^{(01)} = 3.832,\ \kappa_{2,(2)}^{(01)} = 7.016,\ \kappa_{2,(3)}^{(01)} = 10.173, \\ \zeta_2 :\ \zeta_{2,(3,2)}^{(01)} = \frac{10.173}{7.016} = 1.450,\ \zeta_{2,(2,1)}^{(01)} = \frac{7.016}{3.832} = 1.8309,\ \zeta_{2,(3,1)}^{(01)} = \frac{10.173}{3.832} = 2.6547, \\ \kappa_1 :\ \kappa_{1,(1,2,3)}^{(01)} = \frac{3.832 \cdot 7.016}{10.173} = 2.6428, \end{array} \right. \tag{36}$$

that provide multiple suppression of the three first lowest-order scattered-field harmonics of a two-layer impedance GL with the indices $n = 0, \pm 1$, the impedance given by (29), and arbitrary values $\kappa < \kappa_1$ and $\zeta_1 > 1$.

Note that (36) provide the fulfillment of physically grounded relations $\kappa_1 < \kappa_2$ and $\zeta_2 > 1$.

Optics EXPRESS

3.3.2. Comparison of parameters providing multiple suppression for DR, GL, and impedance GL

For a PEC when $\mathbf{w} = \kappa$ consists of one parameter and $D_n^{(1)}(\kappa) = J_n(\kappa)$ the simultaneous suppression of (only) two harmonics with the indices $\pm n$ is possible when $J_n^{(1)}(\nu_m^n) = J_{-n}^{(1)}(\nu_m^n) = 0$, i.e. at $\kappa = \nu_m^n$, where ν_m^n, $m = 1, 2, \ldots$, denote zeros of the nth-order Bessel function $J_n(x)$, $n = 0, 1, 2, \ldots$.

For a bare (single one-layer) dielectric cylinder, a dielectric rod (DR, when the dimensionless parameter vector $\mathbf{w} = (\kappa, \zeta_1)$ comprises two parameters) and GL, vector solutions $\mathbf{w}^*$ to system (12) have been obtained (both in explicit form and numerically) and analyzed in [5]. For a DR it is shown [5] that five scattered-field harmonics with the indices $n = 0, \pm 1, \pm 2$ can be eliminated simultaneously, so that $D_n^{(1)}(\kappa, \zeta_1) = 0$, $n = 0, 1, 2$, if $J_1(\zeta\kappa) = J_1(\kappa) = 0$, i.e. at

$$\begin{cases} \zeta = \zeta_{(l,m)}^{(1)} = \dfrac{\nu_l^1}{\nu_m^1}, \\ \kappa = \kappa_{(m)}^{(1)} = \nu_m^1, \end{cases}, \; l = m+1, m+2, \ldots, \; m = 1, 2, \ldots, \tag{37}$$

where $\zeta = \sqrt{\varepsilon_1}$.

For a 'bare' (standard one-layer) GL (the dimensionless parameter vector $\mathbf{w} = (\kappa, \kappa_1, \zeta_1)$, $\kappa = k_0 a < \kappa_1 = k_0 a_1$), the suppression of two harmonics with the indices $\pm n$ when $D_{-n}^{(1)} = D_n^{(1)} = 0$ ($n = 0, 1, 2, \ldots$) takes place [5] at

$$\begin{aligned} \kappa_1 &= \kappa_{(m)}^{(n)} = \nu_m^n \;\; (n, m = 1, 2, \ldots), \\ \zeta &= \zeta_{(m,s)}^{(n)} = \frac{\nu_s^n}{\nu_m^n} \;\; (n, m, s = 1, 2, \ldots, \; s > m), \\ \kappa &= \kappa_{1,(m,p,s)}^{(n)} = \frac{\nu_p^n \nu_m^n}{\nu_s^n} \;\; (n, m, s, p = 1, 2, \ldots, \; p < s, \; m < s). \end{aligned} \tag{38}$$

One can see that conditions (38) of the GL two-harmonic suppression perfectly match such conditions (35) for a two-layer impedance GL with $n = 1$ if one sets $\kappa_2 = \kappa_1^{GL}$, $\zeta_2 = \zeta^{GL}$, and $\kappa = \kappa_1^{GL}$, so that a two-layer impedance GL with the removed internal dielectric layer ($\kappa = \kappa_1$) behaves like a standard GL.

4. Numerical results and discussion

In the following, numerical examples are presented for two distinct cases: (i) when the first three harmonics are cancelled, and (ii) presentation of similar set of graphs, aiming to put in evidence the non cancellation of the first three harmonics.

The geometry of the configuration under investigation is reported in Fig. 1. The yellow circle (left) and cylinder (right) correspond to the surface impedance, that is located at the interface between the two dielectric layers.

Equations above have been implemented in a Matlab™ script and different parametric analyses have been performed. All simulations have been carried out at $f = 10$ GHz. However, different radii values are reported normalized to the free space wavelengths. In particular, field plots for $\mathbf{E}_{inc} = 1\hat{z}$ (V/m) incident field propagating in the $+\hat{x}$ direction are generated for different number of harmonics n. These later are coded as follows: M corresponds to $2M + 1$ harmonics, i.e., $n = -M, -(M-1), \ldots, -1, 0, 1, \ldots, (M-1), M$. Field has been calculated on a grid of $11\lambda_0 \times 10\lambda_0$ with a step of $0.05\ \lambda_0$ in both directions, i.e., for a total of 221×121 points. For a better monitoring, in the x direction the observation domain starts from $-5\lambda_0$ and extend till $6\lambda_0$, while it is symmetric in the orthogonal y direction. The symmetry axis of the cylinder is identical with the $\hat{z}$ axis, i.e., the central point of the cylinder projection of the (x, y) plane is in the (0,0) point. Considering the observable, value of the scattered field, that is suppose to be low, only amplitude of it has been reported.

Optics EXPRESS

4.1. Case 1: cancellation of three harmonics

The first case refers to the situation when the first three harmonics are cancelled. According to the theoretical values given in (36), it happens for the triplet parameters $\kappa_1 = 2.64233$, $\kappa_2 = 3.83171$, and $\zeta_2 = 2.65508$. As a particular value, $\zeta_1 = 1.55$ has been considered.

Number of harmonics has been increased by pair, i.e., $M = >M + 1$ determines an increase of the number of harmonics from $n = 2M + 1$ to $n = 2(M + 1) + 1$. In Fig. 2 the amplitude of the scattered field for $M = 0$ (one single harmonic) and $M = 1$ (three harmonics) are reported. Referring to the expression of $\tilde{u}^{(L)}(r, \varphi)$ in (5), these corresponds to $l = 0$ and $l = 1$, respectively. In these and following plots, white dashed-line circle represents the metallic cylinder, while the red dashed line indicates the location of the surface impedance Z, positioned at the interface between the two dielectric layers.

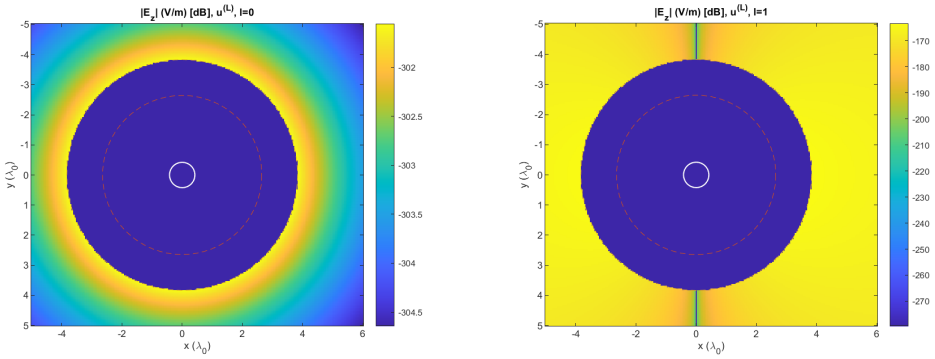

Fig. 2. Scattered electric field amplitude for different number of harmonics: $\tilde{u}^{(L)}(r, \varphi)$ for $l = 0$ (left) and $l = 1$ (right). Note the different scales (values are in dB). The full cancellation of the first harmonic is clear (field level around −300 dB). As for the effect of the addition of the $n = -1$ and $n = 1$ harmonics, the field level of around −200 dB is due to numerical determination of the root of $p_{\pm 1}(w, z)$.

In the following, a value of $M = 10$ has been set in formulas (5). The amplitudes of the different harmonics are presented in Fig. 3 (left), while Fig. 3 (right) reports the corresponding scattered field.

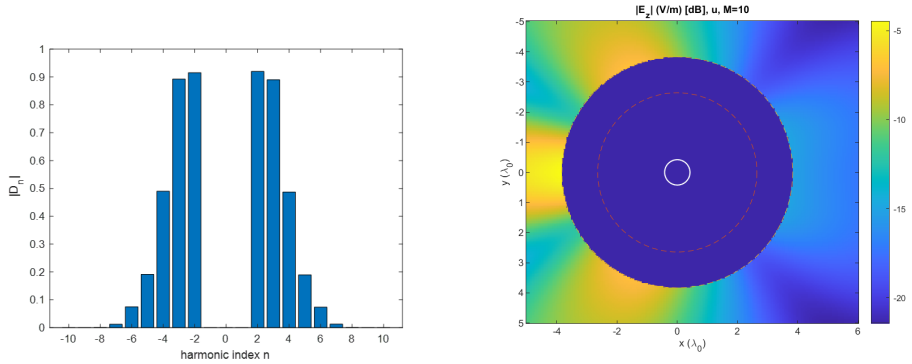

Fig. 3. Case 2: Amplitude D_n of the harmonic indexes for $n = -10, -9, \ldots, -1, 0, 1, \ldots, 9, 10$, corresponding to $M = 10$ (left). Scattered electric field amplitude in dB $\tilde{u}(r, \varphi)$ (right).

Optics EXPRESS

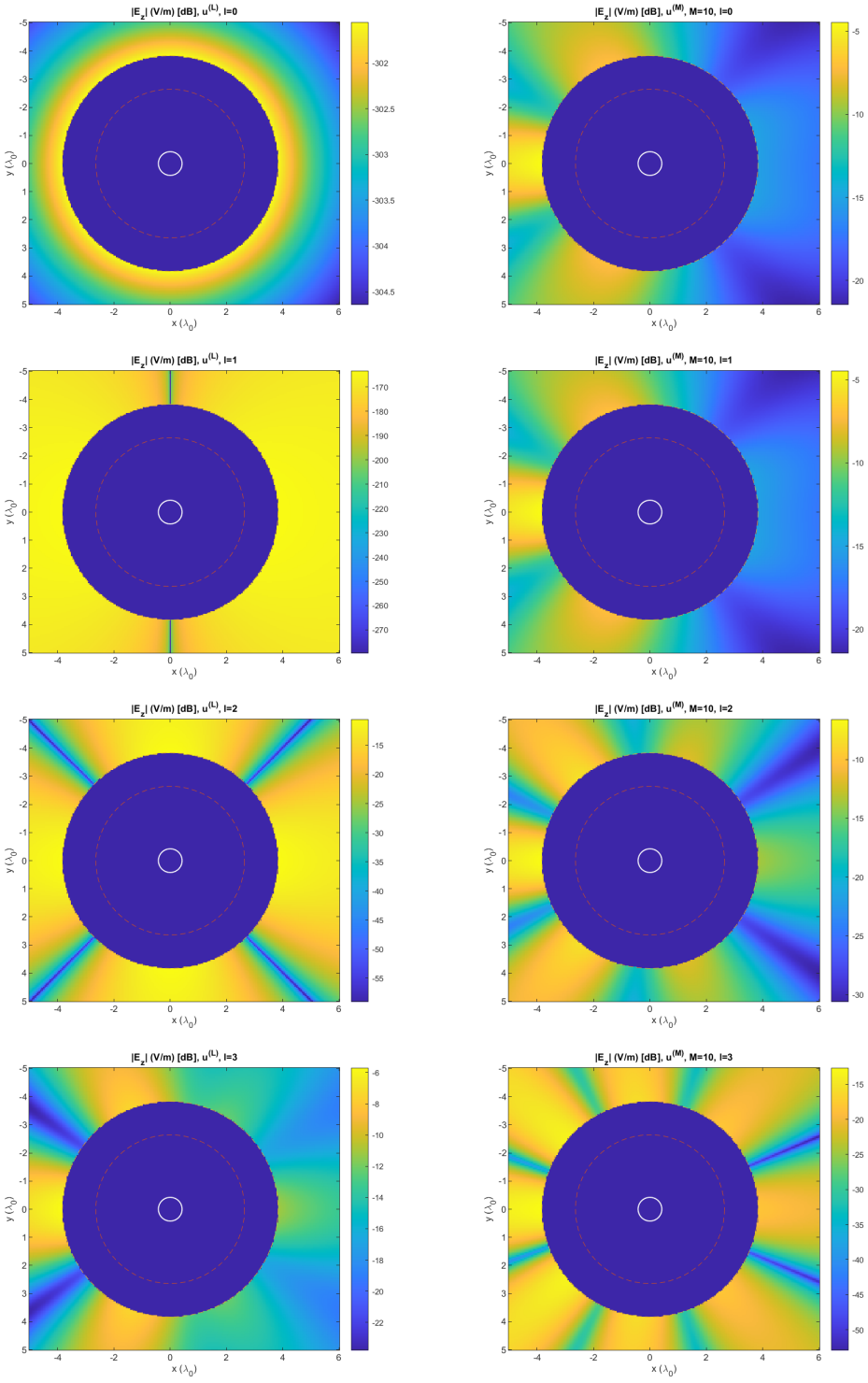

Fig. 4. Scattered electric field amplitude in dB $\tilde{u}^{(L)}(r,\varphi)$ (left) and $\tilde{u}^{(M)}(r,\varphi)$ (right) for different number of harmonics: $M = 10$ and various value of $l = 0 \div 3$. Note the different scales (values are in dB).

Optics EXPRESS

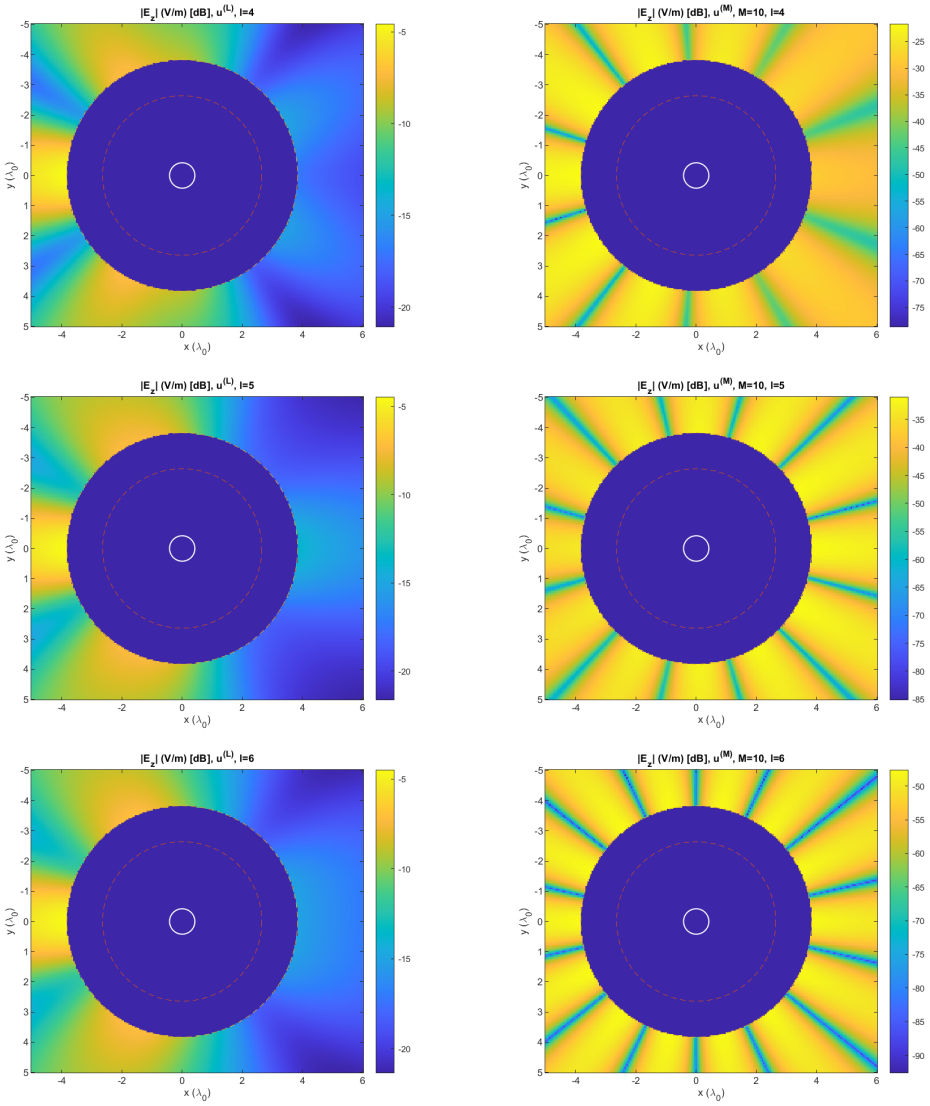

Fig. 5. Scattered electric field amplitude in dB $\tilde{u}^{(L)}(r,\varphi)$ (left) and $\tilde{u}^{(M)}(r,\varphi)$ (right) for different number of harmonics: $M = 10$ and various value of $l = 4 \div 6$. Note the different scales (values are in dB).

Figures 4–6 demonstrate the effect of the single pair of harmonics on the overall scattered field presenting $\tilde{u}^{(L)}(r,\varphi)$ (left) and $\tilde{u}^{(M)}(r,\varphi)$ (right) calculated by (5) for $l \in (0, 9)$. (Separation in three figures is only motivated to give a better rendering and easier referencing.)

Analysing the figures, one can further note, that

- the amplitude of the scattered field presents a "jump" when the first non-evanescent harmonics is considered ($l = 2$ with respect to $l = 1$) as demonstrated in Fig. 4, 2$^{\text{nd}}$ row (left) and 3$^{\text{rd}}$ row (left)

- for all the representations, the field distribution is symmetric with respect to the $\hat{x}$ axis;

Optics EXPRESS

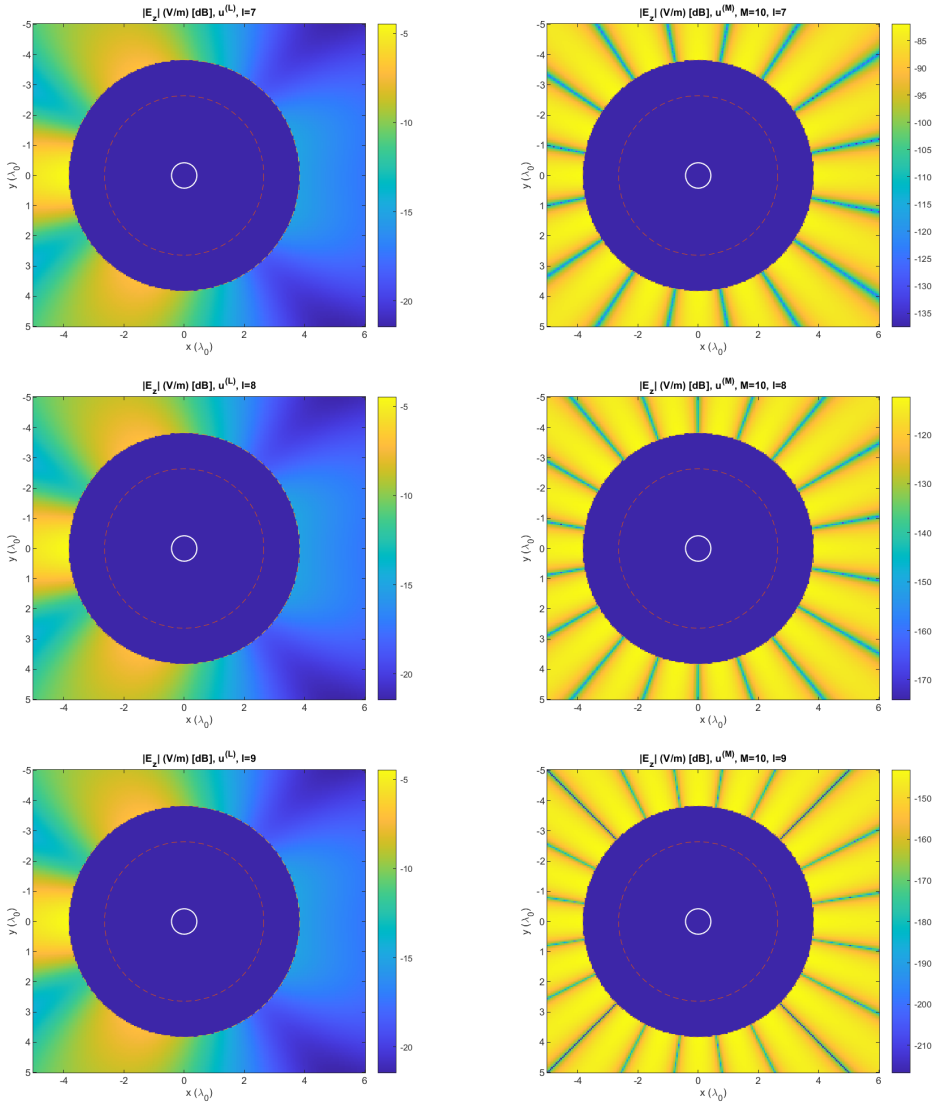

Fig. 6. Scattered electric field amplitude in dB $\tilde{u}^{(L)}(r,\varphi)$ (left) and $\tilde{u}^{(M)}(r,\varphi)$ (right) for different number of harmonics: $M = 10$ and various value of $l = 7 \div 9$. Note the different scales (values are in dB).

- referring to the field amplitude, one can identify that increasing the number of harmonics above $\ell = 3$ (corresponding field plot in Fig. 4, last row, left), does not significantly increase the level of the scattered field in Figs. 5 (left) and 6 (left), but rather concentrates it toward the source (increase of the backscattering) and reduces the field intensity behind the structure. Appearance of the shadow region is visible starting Fig. 4 (last row, left) and it becomes more evident from Fig. 5 (first row, left) onward. The backward radiation is going to be low and more uniform with the increase of the number of harmonics (left columns in Figs. 5 and 6), since local minima of the different terms in the expression of $\tilde{u}(r,\varphi)$ happens at different angles. The field components associated to the harmonic n can be written as:

Optics EXPRESS

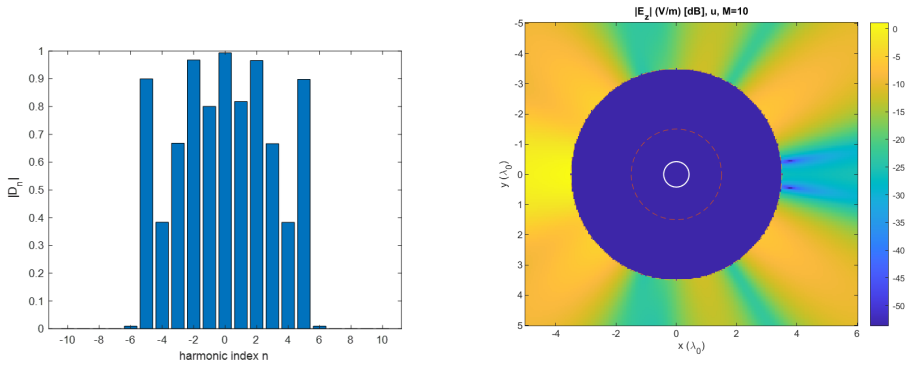

Fig. 7. Case 2: Amplitude D_n of the harmonic indexes for $n = -10, -9, \ldots, -1, 0, 1, \ldots, 9, 10$, corresponding to $M = 10$ (left). Scattered electric field amplitude in dB $\tilde{u}(r, \varphi)$ (right).

$|D_n|\sqrt{J_n^2(k_0 r) + Y_n^2(k_0 r)}\exp\left[\jmath(n\varphi + \arctan\left(\frac{Y_n(k_0 r)}{J_n(k_0 r)}\right) + \arg(D_n))\right]$. Since the amplitude of D_n shows a decreasing behaviour (see Fig. 3, left), such a conclusion has been expected;

- the main contribution comes from the first two non cancelled harmonics, even if the structure is large in terms of wavelength. Such phenomena was not present in [17], where with the increase of the size of the cylinder, the number of harmonics contributing to the scattering increases and the main contribution comes from higher-order terms.

4.2. Case 2: No cancellation of harmonics

To have a better insight of the effect of the simultaneous cancellation of the first three harmonics discussed above, a second configuration has been considered when there is no cancellation of harmonics. The parameters used for this case are $\kappa_1 = 1.5$, $\kappa_2 = 3.5$, and $\zeta_2 = 2.1$.

Actually, this corresponds to the change of the radii of the dielectric layers and the value of the refractive index of the external layer (with respect to the values reported at the beginning of Sec. 4.1). The value of ζ_1 has been maintained the same.

Comparing the spectral composition of the scattered field in Figs. 3 and 7, one can observe a clear difference regarding the amplitude of the $n = -1, 01$ harmonics. In the first case, Fig. 3 (right), they have zero amplitude, while in the second case, Fig. 7 (right), they are almost unitary. The same plots as above have been generated, and presented in Figs. 8, 9 and 10.

Analysing the figures, one can note, that

- the field distribution associated to the firs harmonic is constant in any radial directions (first row Fig. 8, left). This is due to the vanishing argument of the exponential for $n = 0$, hence only the Hankel function is present with a given weight D_0. No one of these factors depend on φ;

- when the number of harmonics increases, minima of the scattered field are for given azimuthal directions, so the directions φ of the minima are due to the exponential term(s). This phenomenon is evincing in all field distributions in Figs. 4–6 and Figs. 8–10, but in the case corresponding to the configuration mentioned at the previous item and when the cancellation of the scattered field has been obtained (first two rows in Fig. 4, left);

- for $l = 5$ one can notice a higher value of the field in the $+\hat{x}$ direction (second last row Fig. 9, left). This is because the amplitude of the 5^{th} harmonics is higher than that of the 4^{th} (Fig. 7

Optics EXPRESS

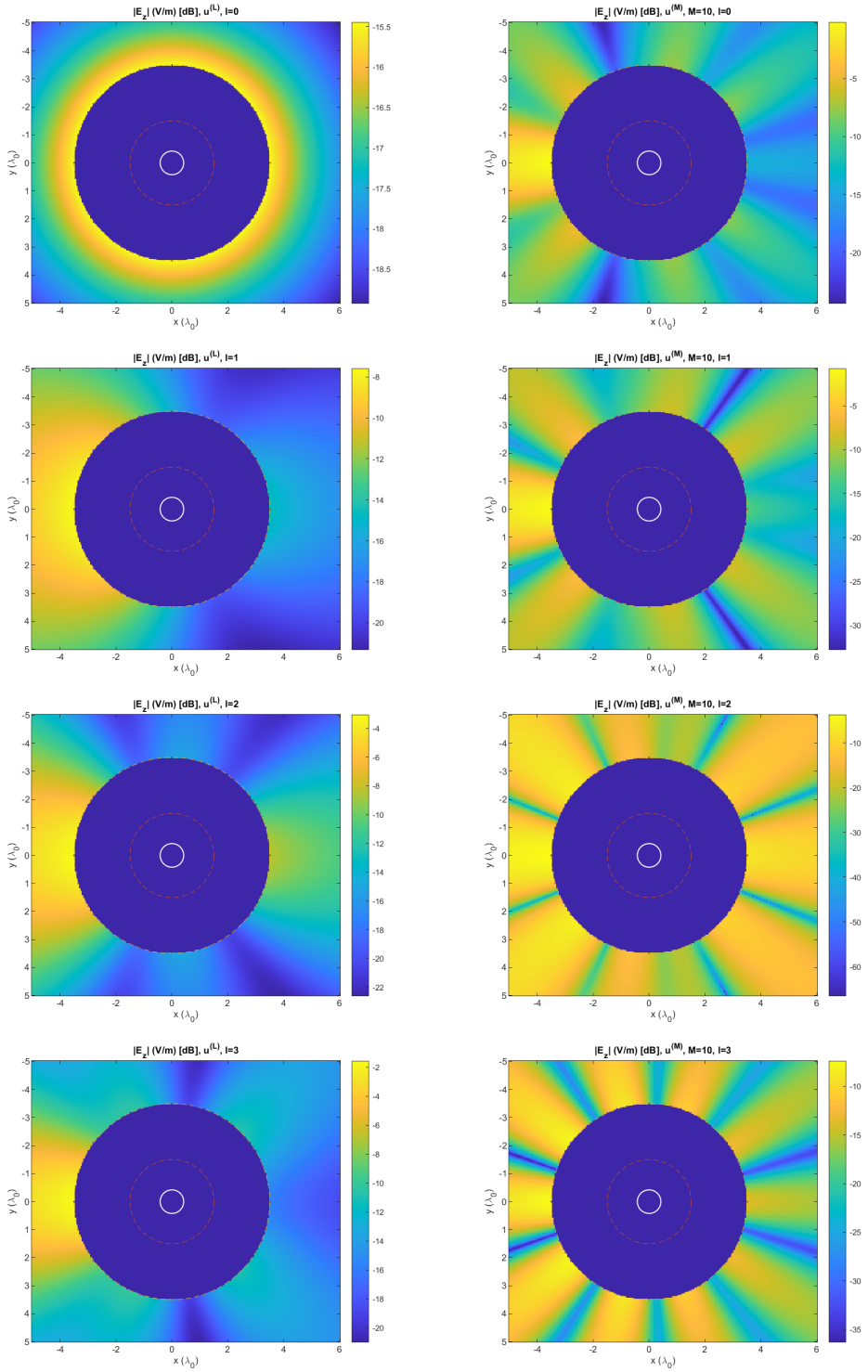

Fig. 8. Scattered electric field amplitude in dB $\tilde{u}^{(L)}(r,\varphi)$ (left) and $\tilde{u}^{(M)}(r,\varphi)$ (right) for different number of harmonics: $M = 10$ and various value of $l = 0 \div 3$. Note the different scales (values are in dB).

Optics EXPRESS

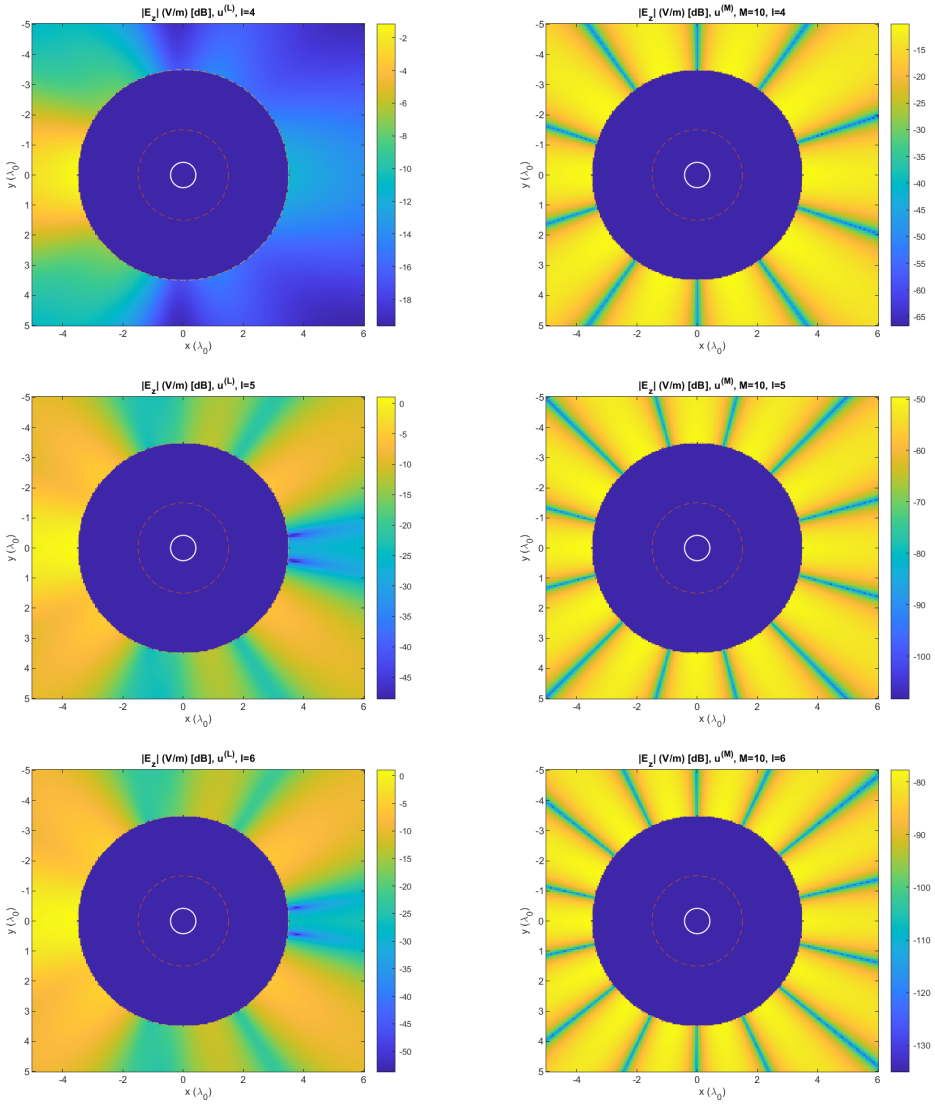

Fig. 9. Scattered electric field amplitude in dB $\tilde{u}^{(L)}(r,\varphi)$ (left) and $\tilde{u}^{(M)}(r,\varphi)$ (right) for different number of harmonics: $M = 10$ and various value of $l = 4 \div 6$. Note the different scales (values are in dB).

right), so when summing it to the other contributions it will be more visible. However this ordering deepens on the selection of the conditions reported at the beginning of this section;

- the increase of the $\tilde{u}^{(L)}(r,\varphi)$ field level for the $l = 5$ terms (discussed above) corresponds a strong decay of the $\tilde{u}^{(M)}(r,\varphi)$: from ≈ -10 dB (first row Fig. 9 (right)) to ≈ -50 dB (second row Fig. 9 (right));

- the contributions of the $n = \pm 6, \pm 7, \pm 8, \pm 9$ harmonic index terms is negligible (this follows from the amplitude of D_n for the considered configuration in Fig. 7 (left)).

Optics EXPRESS

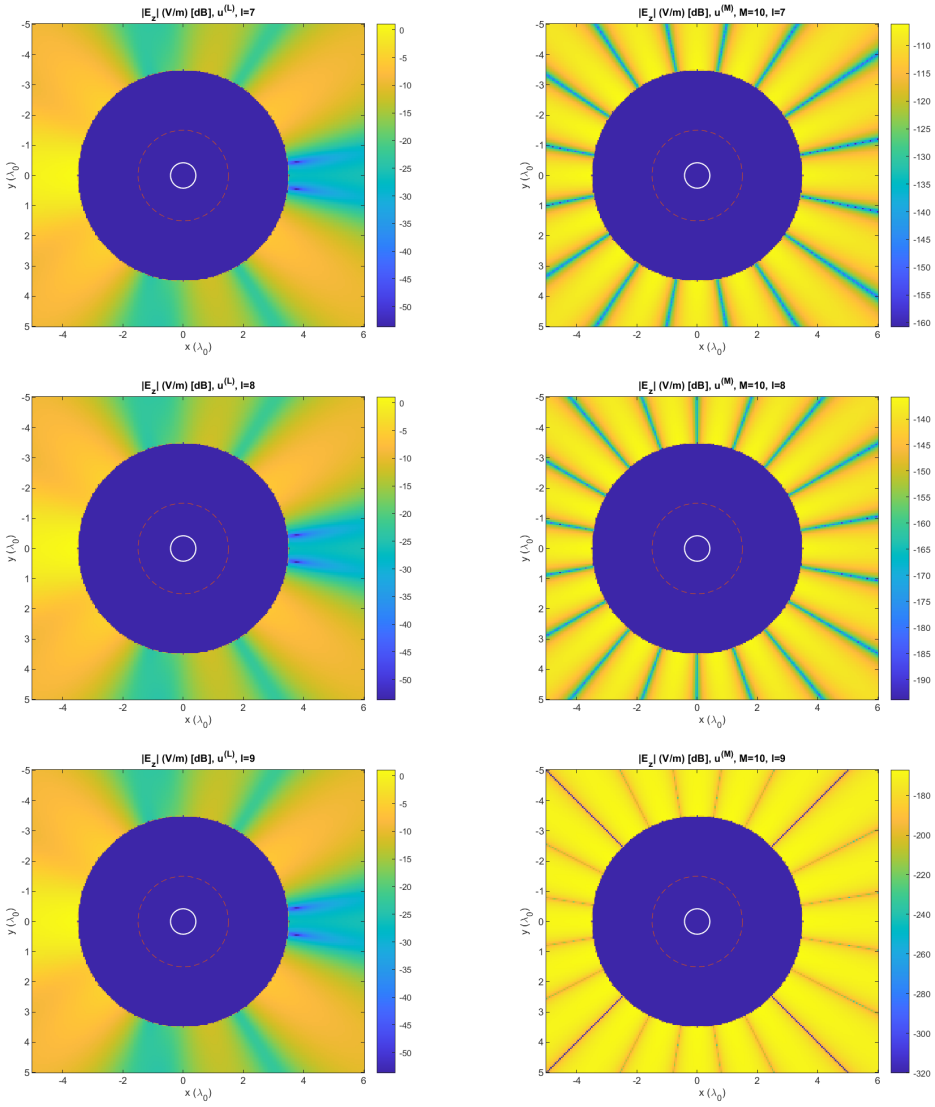

Fig. 10. Scattered electric field amplitude in dB $\tilde{u}^{(L)}(r,\varphi)$ (left) and $\tilde{u}^{(M)}(r,\varphi)$ (right) for different number of harmonics: $M = 10$ and various value of $l = 7 \div 9$. Note the different scales (values are in dB).

5. Concluions

A novel rigorous approach has been elaborated that enables one to determine, for a two-layer impedance GL, explicit numerical values of parameters at which several lowest-order harmonics of the scattered field are cancelled. A detailed visualization and analysis of the partial cloaking achieved as a result of this cancellation have been performed. A characteristic feature of the method is that it provides immediate results for the geometrical and material parameters that yield partial cloaking or invisibility.

Another important feature of the developed technique is that it enables one to increase the number of the suppressed scattered-field harmonics using the impedance as a control parameter.

Optics EXPRESS

A two-layer impedance GL may serve thus as a promising cloaking device with the impedance layer that governs cloaking or invisibility for wider parameter sets and in broader spatial domains.

In particular, the proposed approach and computational tools can be immediately applied to the analysis of the structure comprising a PEC cylinder with the radius much larger than the wavelength because there are no limitations on the range of parameters in the formulas (e.g., (32)) that give the characteristics of suppression.

Note the role of impedance in our analysis: the explicit formulas (30) and (31) have been obtained that couple the impedance with the parameters of the structure (layer permittivities and radii), as well as the inverse relations that couple the parameter values with the impedance, where the range of the varying parameters may be taken arbitrary (as it is mentioned in Sec. 3.3). This result enables one to control the total level of suppression and that of any harmonic by varying either the impedance or the structure parameters. One can state that the obtained explicit formulas for impedance Z of the infinitely thin impedance layer clearly 'summarizes' the suppression (scattering) properties into a single framework providing in this manner a way to understand and verify the main final result of the modeling.

We note that an objective of the present work is to show the possibility of cancelling the given harmonics of the covered cylinder rather than comparing it with the bare cylinder case (hence not only the reduction of the RCS, but the exact mechanism why this happens). The results presented in the figures demonstrate several different aspects of the achieved suppression.

The method, including its theoretical approach and computational tools, can be extended to any dielectric-layered impedance structures possessing circular or planar symmetry.

The developed approach is a rigorous method that enables one to obtain explicit values of parameters (without numerical calculations) that provide the cloaking effect, particularly in terms of the suppression of the scattered field harmonics and variation of the sheet impedance. This issue constitutes the novelty of the performed study and the reported findings. In this respect, the elaborated technique can be used to validate the results obtained by commercial solvers as well as to study more complicated multi-layer mantle cloaks with ot without impedance sheets and with no limitations on the range of parameters.

6. Appendix: Cross-products of cylindrical functions

According to the definition [18], 9.1.33 (and preserving the original notations), the expressions

$$p_n = p_n(x,y) = J_n(x)\,Y_n(y) - J_n(y)\,Y_n(x) = \begin{vmatrix} J_n(x) & Y_n(x) \\ J_n(y) & Y_n(y) \end{vmatrix}, \tag{39}$$

$$q_n = q_n(x,y) = J_n(x)\,Y_n'(y) - J_n'(y)\,Y_n(x) = \begin{vmatrix} J_n(x) & Y_n(x) \\ J_n'(y) & Y_n'(y) \end{vmatrix}, \tag{40}$$

$$r_n = r_n(x,y) = J_n'(x)\,Y_n(y) - J_n(y)\,Y_n'(x) = \begin{vmatrix} J_n'(x) & Y_n'(x) \\ J_n(y) & Y_n(y) \end{vmatrix}, \tag{41}$$

$$s_n = s_n(x,y) = J_n'(x)\,Y_n'(y) - J_n'(y)\,Y_n'(x) = \begin{vmatrix} J_n'(x) & Y_n'(x) \\ J_n'(y) & Y_n'(y) \end{vmatrix}, \tag{42}$$

Optics EXPRESS

are called cross-products of the nth-order Bessel and Neumann functions $J_n(x)$ and $Y_n(x)$ and their derivatives $J_n'(x)$ and $Y_n'(x)$, $n = 0, 1, 2, \ldots$. In particular,

$$\begin{aligned} q_0 &= I_{1,0}(y,x) = J_1(y)\,Y_0(x) - J_0(x)\,Y_1(y), \\ r_0 &= I_{0,1}(y,x) = -I_{1,0}(x,y) = J_0(y)\,Y_1(x) - J_1(x)\,Y_0(y), \\ s_0 &= p_1 = J_1(x)\,Y_1(y) - J_1(y)\,Y_1(x), \end{aligned} \tag{43}$$

Cross-products have been a subject of intense studies [19–23], particularly, using the technique [20] which enables highly accurate calculation of zeros. Note that the recently developed approach [19] facilitates the analysis of weighted cylindrical polynomials considered as a genaralization of cross-products.

Present the essential information concerning the occurrence of (real) zeros of cross-products $p_n = p_n(y)$ given by (39) considered as functions of y:

- For every $x>0$ functions $p_n(y)$, $n = 0, 1, 2, \ldots$, has each infinitely many positive zeros $p_m^n = p_m^n(x)$, $n = 0, 1, 2, \ldots$, $m = 1, 2, \ldots$, alternating with zeros of $J_n(y)$ and $Y_n(y)$ (see Figs. 11).
- Any root $p_m^n(x)$ is a continuous increasing function of $x>0$.
- $p_n(y = x) = 0$, i.e. all $p_n(y)$, $n = 0, 1, 2, \ldots$, have the same zero $p_0^{n,*} = x$ and for every $x>0$, $\{p_m^n(x)\}_{m=1}^{\infty}$ is virtually a periodic sequence with the same period π as the zeros of J_n and

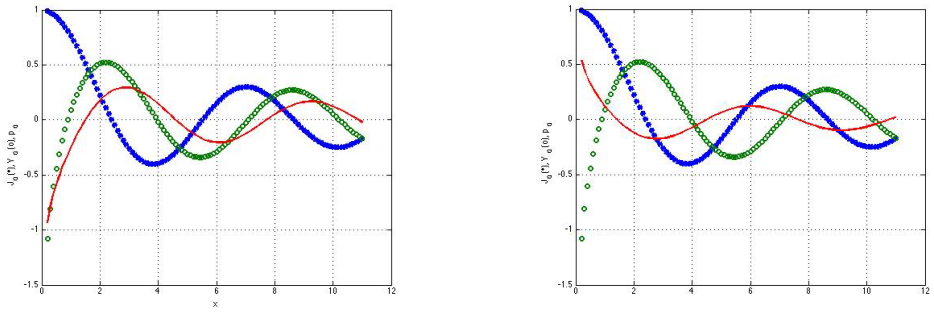

Fig. 11. Plots of $J_0(y)$ (*), $Y_0(y)$ (o), and $p_0(y)$ (-) at $x = 1.5$ (left) and $x = 4.5$ (right).

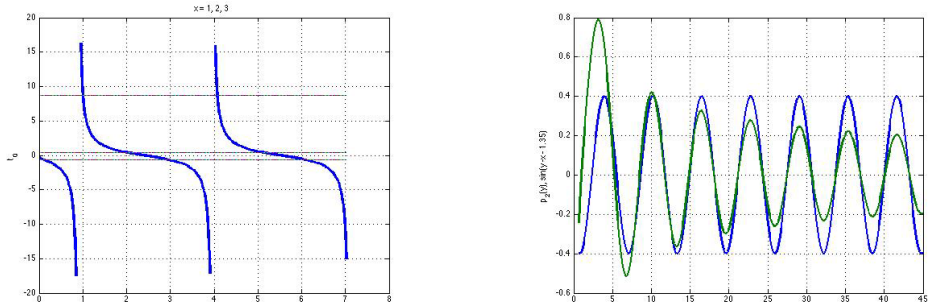

Fig. 12. Left: plots of $t_0(y) = \dfrac{J_0(y)}{Y_0(y)}$ and the lines $t_0(x) = \dfrac{J_0(x)}{Y_0(x)}$, $x = 1, 2, 3$ (upper, middle, and lower lines). Right: $p_2(y)$ and $0.4\sin(y - x - 1.35)$ at $x = 1$.

Optics EXPRESS

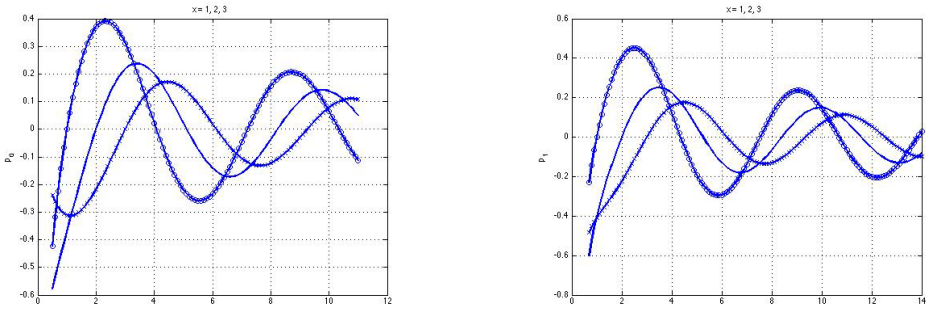

Fig. 13. Plots of $p_0(y)$ (left) and $p_1(y)$ (right) at $x = 1$ (o), $x = 2$ (-), and $x = 3$ (*).

Y_n have, so that, highly accurate,

$$p^n_{m+1} = p^n_1 + x + m\pi, \quad m = 1, 2, \ldots, \; n = 0, 1, 2, \ldots \tag{44}$$

(see Fig. 12 and Fig. 13).

Funding. Unitatea Executiva pentru Finantarea Invatamantului Superior, a Cercetarii, Dezvoltarii si Inovarii (PN-III-P4-ID-PCE-2020-0404).

Disclosures. The authors declare no conflicts of interest.

Data availability. No data were generated or analyzed in the presented research.

References

1. A. Alú and N. Engheta, "Achieving transparency with plasmonic and metamaterial coatings," Phys. Rev. E **72**(1), 016623 (2005).
2. U. Leonhardt, "Optical conformal mapping," Science **312**(5781), 1777–1780 (2006).
3. J. B. Pendry, D. Schurig, and D. R. Smith, "Controlling electromagnetic fields," Science **312**(5781), 1780–1782 (2006).
4. A. Alú, "Mantle cloak: invisibility induced by a surface," Phys. Rev. B **80**(24), 245115 (2009).
5. Y. Shestopalov, "Cloaking: Analytical Theory for Benchmark Structures," J. Electromagn. Waves Appl. **35**(4), 485–510 (2021).
6. Y. Shestopalov, E. Kuzmina, and A. Samokhin, "On a Mathematical Theory of Open Metal–Dielectric Waveguides," *FERMAT*, 2014. Open access: https://www.e-fermat.org/files/articles/153bac073a019f.pdf
7. Y. Shestopalov, "Resonance Scattering by a Circular Dielectric CylinderShestopalov," Radio Sci. **56**(6), e2020RS007095 (2021).
8. Z. Jacob, L. V. Alekseyev, and E. Narimanov, "Optical Hyperlens: Far-field imaging beyond the diffraction limit," Opt. Express **14**(18), 8247 (2006).
9. Y. Taguchi, Y. Takahashi, Y. Sato, T. Asano, and S. Noda, "Statistical studies of photonic heterostructure nanocavities with an average Q factor of three million," Opt. Express **19**(12), 11916 (2011).
10. J. Pendry, "Perfect cylindrical lenses," Opt. Express **11**(7), 755 (2003).
11. C. M. Bingham, H. Tao, X. Liu, R. D. Averitt, X. Zhang, and W. J. Padilla, "Planar wallpaper group metamaterials for novel terahertz applications," Opt. Express **16**(23), 18565 (2008).
12. O. M. Bucci and G. Franceschetti, "On the degrees of freedom of scattered fields," IEEE Trans. Antennas Propag. **37**(7), 918–926 (1989).
13. G. Labate and L. Matekovits, "Invisibility and Cloaking Structures as Weak or Strong Solutions of Devaney-Wolf Theorem," Opt. Express **24**(17), 19245–19253 (2016).
14. Z. Hamzavi-Zarghani, A. Yahaghi, L. Matekovits, and A. Farmani, "Tunable Mantle Cloaking Utilizing Graphene Metasurface for Terahertz Sensing Applications," Opt. Express **27**(24), 34824–34837 (2019).
15. G. Labate, S. K. Podilchak, and L. Matekovits, "Closed-form Harmonic Contrast Control with Surface Impedance Coatings for Conductive Objects," Appl. Opt. **56**(36), 10055–10059 (2017).
16. G. Labate, A. K. Ospanova, N. A. Nemkov, Al. A. Basharin, and L. Matekovits, "Nonradiating Anapole Condition Derived from Devaney-Wolf Theorem and Excited in a Broken-Symmetry Dielectric Particle," Opt. Express **28**(7), 10294–10307 (2020).
17. B. Cappello and L. Matekovits, "Harmonic analysis and reduction of the scattered field from electrically large cloaked metallic cylinders," Appl. Opt. **59**(12), 3742–3750 (2020).
18. M. Abramowitz and I. Stegun, *Handbook of Mathematical Functions* (Dover, New York, 1972).

Optics EXPRESS

19. Y. Shestopalov, "Trigonometric and cylindrical polynomials and their applications in electromagnetics," Appl. Anal. **99**(16), 2807–2822 (2020).
20. M. K. Kerimov, "Investigations on zeros of special Bessel functions," Zh. Vychisl. Mat. Mat. Fiz. **54**(9), 1387–1441 (2014).
21. D. Kirkham, "Graphs and Formulas for Zeros of Cross Product Bessel Functions," J. Math Phys. **36**(1-4), 371–377 (1957).
22. Math. Tables and Aids to Computations (MTAC), 1:222; 2:37, 173; 3:305; 6:24-25; 7:280; 8:223 (1943–1954).
23. J. M. Ek, H. P. Thielman, and E. C. Huebschman, "On the Zeros of Cross-Product Bessel Functions," Journal of Mathematics and Mechanics **16**(5), 447–452 (1966).